

# Retroactivity Attenuation in Transcriptional Networks: Design and Analysis of an Insulation Device

Domitilla Del Vecchio and Shridhar Jayanthi

**Abstract**—Retroactivity is a phenomenon that changes the desired input/output response of a system when it is connected to “downstream” systems. Transcriptional networks are not immune to this phenomenon. In this paper, we propose a phosphorylation-based design for a bio-molecular system that acts as an insulator between its upstream systems and its downstream ones in a transcriptional network. Performing singular perturbation analysis, we mathematically show that such a design attenuates retroactivity. Stochastic simulations are run to analyze the robustness of the proposed device to biological noise and to highlight design tradeoffs.

## I. INTRODUCTION

The concept of retroactivity generalizes the notion of impedance to non-electric systems. It basically describes the amount by which the I/O response of a system is affected by interconnections. As in electrical, hydraulic, and mechanical systems, also in bio-molecular systems this phenomenon covers an important role. This is the case both for *synthetic* biological systems that are modularly designed [1], and for natural biological networks that are modularly analyzed [9]. Modular analysis and design is possible only if “modules” maintain their functions unchanged upon interconnection. Therefore, it is important to quantify retroactive effects in these biological systems and to identify mechanisms to isolate them. The notion of retroactivity has been introduced in the context of bio-molecular systems by [16] and it has been mathematically characterized for transcriptional networks by the author and co-workers prior work [6].

In this paper, we briefly review the formal definition of retroactivity proposed in [6] and we focus on the design of devices that can be placed between two modules to isolate them from retroactive effects. The understanding of fundamental design principles of bio-molecular insulation devices is crucial both in synthetic and in natural systems. This understanding enables the retroactive-free interconnection of synthetic components and is central to uncover the directionality of signal propagation in natural networks. The idea of a bio-molecular insulation device based on the non-inverting amplifier design has been explored to some extent [6], [17]. In this paper, we provide a general theoretical treatment of the design of bio-molecular insulation devices based on time-scale separation properties. We show how the attenuation of the retroactivity can be realized in a bio-

molecular device by speeding up its dynamics with respect to its input.

Based on our theoretical development, which employs singular perturbation techniques, we show how an insulation device based on a phosphorylation cycle has an intrinsic insulation property. This is due to its fast time-scale when compared to protein production and decay processes. Phosphorylation/dephosphorylation systems have been shown to play different roles in cells such as fast amplification of signals in the visual system [18], regulating metabolic and signaling pathways [12] and triggering mechanical response [4]. The new insulation property of phosphorylation cycles highlights another potential reason why they are ubiquitous in natural signal transduction systems: they can isolate the system that sends the signal from the one that receives the signal. This allows faithful signal propagation. In this system, having a fast time-scale is qualitatively equivalent to having large input amplification and large negative feedback gains. Since there is extensive work witnessing the sensitivity of the noise properties of a bio-molecular system to increase in feedback gain (see [3], [10], for example), we analyze the noise properties of the phosphorylation cycle when the gains are changed. This is performed numerically by employing Gillespie’s Stochastic Simulation Algorithm (SSA) [7]. An increase of these gains attenuates more the retroactive effects but also increases the coefficient of variation of the species. This highlights a potential design trade-off between the insulation capability and sensitivity to biological noise.

In Section II, we revise the notion of retroactivity from a control systems point of view. In Section III, we propose a theoretical framework for the design of insulation devices. In Section IV, we show the realization of an insulation device based on a phosphorylation cycle. In Section V, we analyze the sensitivity to biological noise when the internal gains of the device are changed.

## II. RETROACTIVITY IN TRANSCRIPTIONAL NETWORKS

### A. The Retroactivity Concept

The concept of retroactivity broadly encompasses loading effects arising at interconnections in electrical, hydraulic, mechanical, and biological systems. Upon interconnection between an upstream system and a downstream system, the dynamics of the internal state and of the output of the upstream system changes. This phenomenon can be modeled by a signal that travels from downstream to upstream, which we call retroactivity. The amount of such a retroactivity will change depending on the features of the interconnection and of the downstream system. We thus represent a system

D. Del Vecchio and S. Jayanthi are with the Department of Electrical Engineering and Computer Science at the University of Michigan, Ann Arbor, MI 48109. The authors would like to thank Eduardo D. Sontag and Alexander J. Ninfa for discussions that were relevant to the development of this paper.

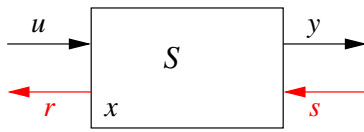


Fig. 1. A system model with retroactivity.

according to the diagram shown in Figure 1 as proposed in [6]. An input is added, called  $s$ , to the system to model any change in its dynamics that may occur upon interconnection with a downstream system. Similarly, a signal  $r$  is added as another output, to model the fact that when such a system is connected downstream of another system, it will send upstream a signal that will alter the dynamics of the upstream system. A system  $S$  is thus defined to have internal state  $x$ , two types of inputs (I), and two types of outputs (O): an input “ $u$ ” (I), an output “ $y$ ” (O), a *retroactivity to the input* “ $r$ ” (O), and a *retroactivity to the output* “ $s$ ” (I) (Figure 1). We represent such a system  $S$  by the equations

$$\frac{dx}{dt} = f(x, u, s), \quad y = Y(x, u, s), \quad r = R(x, u, s), \quad (1)$$

in which  $f, Y, R$  are arbitrary functions and the signals  $x, u, s, r, y$  may be scalars or vectors. In this formalism, we define the input/output model of the isolated system as the one in equations (1) without  $r$  in which we have also set  $s = 0$ . This model generalizes the standard input/output formalism of control theory, while it can be still viewed as a special case of the behavioral models [15].

From a design point of view, having a system whose dynamics is affected by  $s$  and that outputs a non zero  $r$  is undesirable. In fact, especially in circuit design and in control systems, an input/output device is usually designed in isolation to have a desired input/output response. Such a desired response should be maintained despite whether the device is interconnected, in order to design and analyze complex systems in a modular fashion. Since this same modular approach to design and analysis of networks is taken in synthetic and systems biology, we investigate the amounts of these retroactivity effects in transcriptional networks.

### B. Transcriptional Networks are Affected by Retroactivity

The retroactivity concept in the context of bio-molecular systems has been considered also by other authors [16]. Their approach is to re-partition inputs and outputs of a chemical network to minimize the amounts of retroactivity. Our approach instead considers fixed inputs and outputs and focuses on the design of devices that can be placed between an upstream system and a downstream one to isolate them. A transcriptional network is composed by a number of genes that express proteins that then act as transcription factors for other genes. Such a network can be generally represented as nodes connected by directed edges. Each node represents a gene and each arrow from node  $z$  to node  $x$  indicates that the transcription factor encoded in  $z$ , denoted  $Z$ , regulates gene  $x$  [1]. In this paper, we model each node  $x$  of the network as an input/output module taking as input the transcription factors

that regulate gene  $x$  and as output the protein expressed by gene  $x$ , denoted  $X$ . A directed edge between nodes  $z$  and  $x$  indicates that protein  $Z$  binds to the operator sites of gene  $x$  to alter (repress or activate) the expression of the latter. We denote by  $X$  the protein, by  $X$  (italics) the average protein concentration, and by  $x$  (lower case) the gene expressing protein  $X$ . A transcriptional component that takes as input protein  $Z$  and gives as output protein  $X$  is shown in Figure 3 in the dashed box. The activity of the promoter controlling

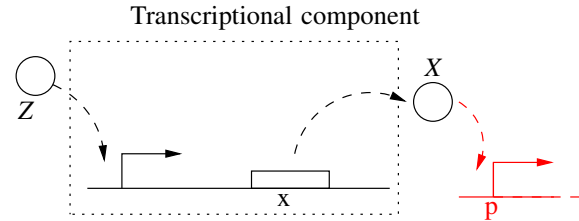


Fig. 3. The transcriptional component takes as input  $u$  protein concentration  $Z$  and gives as output  $y$  protein concentration  $X$ . The transcription factor  $Z$  binds to operator sites on the promoter. The red part belongs to a downstream transcriptional block that takes protein concentration  $X$  as its input.

gene  $x$  depends on the amount of  $Z$  bound to the promoter. If  $Z = Z(t)$ , such an activity changes with time. We denote it by  $k(t)$ . By neglecting the mRNA dynamics, we can write the dynamics of  $X$  as

$$\frac{dX}{dt} = k(t) - \delta X, \quad (2)$$

in which  $\delta$  is the decay rate of the protein. We refer to equation (2) as the isolated system dynamics. The reversible binding reaction of  $X$  with  $p$  is given by  $X + p \xrightleftharpoons[k_{off}]{k_{on}} C$ , in which  $C$  is the complex protein-promoter and  $k_{on}$  and  $k_{off}$  are the binding and dissociation rates of the protein  $X$  to the promoter site  $p$ . Since the promoter is not subject to decay, its total concentration  $p_{TOT}$  is conserved so that we can write  $p + C = p_{TOT}$ . Therefore, the new dynamics of  $X$  is governed by the equations

$$\begin{aligned} \frac{dX}{dt} &= k(t) - \delta X + \boxed{k_{off}C - k_{on}(p_{TOT} - C)X}, \\ \frac{dC}{dt} &= -k_{off}C + k_{on}(p_{TOT} - C)X. \end{aligned} \quad (3)$$

The terms in the box represent the signal  $s$ , that is, the retroactivity to the output, while the second of equations (3) describes the dynamics of the input stage of the downstream system driven by  $X$ . Then, we can interpret  $s$  as a mass flow between the upstream and the downstream system. When  $s = 0$ , the first of equations (3) reduces to the dynamics of the isolated system given in equation (2). Figure 2 shows the dramatic effect of the retroactivity to the output  $s$  on the dynamics of the transcriptional module. A mathematical framework for quantifying the retroactivity effect on the dynamics has been proposed in [6].

Since the load  $p$  cannot necessarily be designed to generate a small retroactivity, we instead design a device that can be placed between the transcriptional component and its load to isolate  $X$  from retroactive effects.

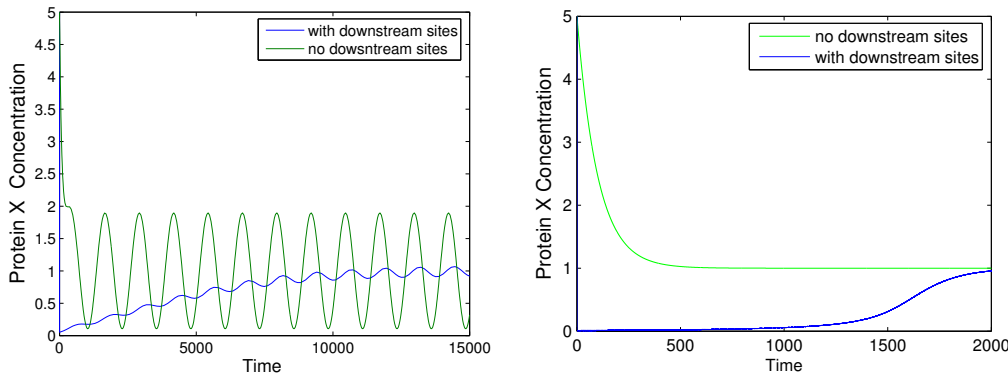


Fig. 2. The dramatic effect of interconnection. Simulation results for the system in equations (3). Here,  $k(t) = 0.01(1 + \sin(\omega t))$  in the left plot and  $k(t) = 0.01$  in the right side plot. Also,  $\omega = 0.005$ ,  $k_{on} = 10$ ,  $k_{off} = 10$ ,  $\delta = 0.01$ ,  $p_{TOT} = 100$ ,  $X(0) = 5$ . The protein decay rate (in  $\text{min}^{-1}$ ) corresponds to a half life of about one hour. The frequency of oscillations has a period of about 12 times the protein half life in accordance to what is experimentally observed in [2]. The green plot (solid line) represents  $X(t)$  originating by equations (2), while the blue plot (dashed line) represents  $X(t)$  obtained by equation (3). Both transient and permanent behaviors are different.

### III. A TIME-SCALE SEPARATION APPROACH TO THE DESIGN OF BIO-MOLECULAR INSULATION DEVICES

We define an *insulation device* as a system with the structure shown in Figure 1 for which (i)  $r \ll 1$ ; (ii)  $s$  is almost completely attenuated; (iii) the input/output response is linear in the signal range of interest. We next show that a bio-molecular system whose internal dynamics evolves on a fast time scale compared to the input can also attenuate the retroactivity to the output. Singular perturbation techniques are employed to show this property.

We consider a system  $S$  as shown in Figure 1, in which we make the following structural assumptions:

- (i) The variables  $r, s$  are scalars,  $u, y \in \mathbb{R}_+$ ,  $x = (x_1, \dots, x_n) \in \mathcal{D} \subseteq \mathbb{R}_+^n$  and  $y = x_n$ ;
- (ii)  $r$  and  $s$  enter the dynamics as *additive rates* and they affect only the dynamics of the  $u$  and  $y$  variables, respectively, that is,

$$\frac{du}{dt} = f_0(t, u) + r(x, u) \quad (4)$$

and  $\frac{dx_n}{dt} = Gf_n(x) + s(v, y)$ , in which  $G > 0$  and  $v = (v_1, \dots, v_p) \in \mathbb{R}_+^p$  is the internal state variable of the downstream system whose dynamics is given by

$$\frac{dv}{dt} = \begin{pmatrix} g_1(v, y) \\ g_2(v) \\ \vdots \\ g_p(v) \end{pmatrix}; \quad (5)$$

- (iii) The internal dynamics of system  $S$  once it is connected to its downstream system is given by

$$\frac{dx}{dt} = \begin{pmatrix} Gf_1(x, u) \\ Gf_2(x) \\ \vdots \\ Gf_{n-1}(x) \\ Gf_n(x) + s(v, y) \end{pmatrix}; \quad (6)$$

- (iv) The following conservation laws for the retroactivity rates hold:  $r(x, u) = -Gf_1(x, u)$ , and  $s(v, y) = -g_1(v, y)$ .

Property (iv) models the retroactivity as a flow through the interconnection from the downstream system to the upstream one. From a biological point of view, this property is satisfied in interconnection mechanisms that occur through protein/protein or protein/promoter binding/unbinding. More general models could be considered in which  $r$  and  $s$  are vectors and they enter the dynamics of multiple variables in their corresponding upstream systems. The constant  $G$  in equations (6) is a gain. In the special case in which  $x \in \mathbb{R}$  and  $f_1(x, u) = au - \beta x$ ,  $G$  plays exactly the role of an input gain and of a negative feedback gain. The parameter  $G$  also quantifies the speed of the dynamics of system  $S$ . We seek to show that as  $G$  increases, under suitable stability assumptions, the effect of the retroactivity to the output  $s$  on the dynamics of  $S$  becomes negligible after a short initial transient. Also, the retroactivity to the input  $r$  can be measured as a static function of the input  $u$  to  $S$  and of the internal parameters of  $S$ .

**Assumption 1:** Define the function  $F : \mathbb{R}_+ \times \mathcal{D} \rightarrow \mathbb{R}^n$  by  $F(a, x) := (f_1(x, a - x_1), f_2(x), \dots, f_n(x))$ ,  $a \in \mathbb{R}_+$ , and  $x \in \mathcal{D}$ . We assume that all the eigenvalues of  $\frac{\partial F}{\partial x}(a, x)$  have negative real parts for all  $x \in \mathcal{D}$  and all  $a \in \mathcal{D}' := \{a \in \mathbb{R}_+ \mid a - x_1 \geq 0, x \in \mathcal{D}\}$ .

**Claim 1:** Let  $x(t)$  be generated by system (4-5-6) and let  $x^{ref}(t)$  be generated by the same system where we have set  $s(v, y) = 0$ . Then, there exist constants  $G^*, t_0, T > 0$  such that  $\|x^{ref}(t) - x(t)\| = \mathcal{O}(1/G)$  for all  $t \in [t_0, T)$  and all  $G > G^*$ .

*Proof:* Employ the change of variables  $\tilde{u} := u + x_1$ ,  $\tilde{x}_n = x_n + v_1$ , and set  $\epsilon := 1/G$ . The dynamics of system (4-5-6) in these new variables become

$$\begin{aligned} \frac{d\tilde{u}}{dt} &= f_0(t, \tilde{u} - x_1) \\ \epsilon \frac{d\tilde{x}_1}{dt} &= f_1(x_1, \dots, x_{n-1}, \tilde{x}_n - v_1, \tilde{u} - x_1) \end{aligned}$$

$$\begin{aligned}
\epsilon \frac{dx_i}{dt} &= f_i(x_1, \dots, x_{n-1}, \bar{x}_n - v_1), \text{ for } 1 < i < n \\
\frac{d\bar{x}_n}{dt} &= f_n(x_1, \dots, x_{n-1}, \bar{x}_n - v_1) \\
\frac{dv_1}{dt} &= g_1(v, \bar{x}_n - v_1).
\end{aligned} \tag{7}$$

For  $\epsilon \ll 1$ , the above system is in standard singular perturbation form. Setting  $\epsilon = 0$ , one can compute the slow manifold, which, in the  $(x, \bar{u})$  variables is given by  $\{(x, \bar{u}) \mid x = \gamma(\bar{u}), \text{ with } \gamma(\bar{u}) \text{ locally unique solution of } F(\bar{u}, \gamma(\bar{u})) = 0\}$ . Denote  $\gamma(\bar{u}) = (\gamma_1(\bar{u}), \dots, \gamma_n(\bar{u}))$ . Since all the eigenvalues of  $\frac{\partial F}{\partial x}(\bar{u}, x)$  have negative real parts, the trajectories are attracted to the slow manifold. Thus, we can apply the singular perturbation theorem on the finite time interval [14] to conclude that there are  $\epsilon_1^*, t_0', T' > 0$  such that  $x(t) = \gamma(\bar{u}(t)) + O(\epsilon)$  for all  $\epsilon < \epsilon_1^*$  and  $t \in [t_0', T']$ , in which  $\bar{u}$  is given by  $d\bar{u}/dt = f_0(t, \bar{u} - \gamma_1(\bar{u}))$ . This expression of  $x(t)$  does not depend on the values of  $v$ . Consider now  $x^{ref}(t)$  as generated by (4-5-6) in which  $s(v, y) = 0$ . Employing the change of variables  $\bar{u} := u + x_1$  and setting  $\epsilon := 1/G$ , the dynamic of  $S$  becomes

$$\begin{aligned}
\frac{d\bar{u}}{dt} &= f_0(t, \bar{u} - x_1^{ref}) \\
\epsilon \frac{dx_1^{ref}}{dt} &= f_1(x_1^{ref}, \bar{u} - x_1^{ref}), \quad \epsilon \frac{dx_i^{ref}}{dt} = f_i(x_1^{ref}), \text{ for } 1 < i \leq n.
\end{aligned}$$

By setting  $\epsilon = 0$  and computing the slow manifold, one obtains the same solution  $x^{ref} = \gamma(\bar{u})$  as obtained earlier. Therefore, there are  $\epsilon_2^*, t_0'', T'' > 0$  such that  $x^{ref}(t) = \gamma(\bar{u}(t)) + O(\epsilon)$  for all  $\epsilon < \epsilon_2^*$  and  $t \in [t_0'', T'']$ . Setting  $G^* := 1/\min(\epsilon_1^*, \epsilon_2^*)$ ,  $t_0 := \max(t_0', t_0'')$ , and  $T := \min(T', T'')$ , the desired result follows. ■

This result indicates that an input/output bio-molecular system that evolves on a faster time-scale than its input is likely to attenuate very well the retroactivity to its output.

**Claim 2:** Let  $u(t)$  be generated by system (4-5-6). Set  $f(a, x) := (f_1(x, a), f_2(x), \dots, f_n(x))$  and assume that  $f(a, \gamma(a)) = 0$  admits a unique solution  $\gamma : \mathbb{R}_+ \rightarrow \mathbb{R}^n$  with  $\gamma(a) = (\gamma_1(a), \dots, \gamma_n(a))$  and  $\gamma_i : \mathbb{R}_+ \rightarrow \mathbb{R}_+$ . Let  $\bar{u}(t) \in \mathbb{R}_+$  be generated by the system

$$\frac{d\bar{u}}{dt} = f_0(t, \bar{u}) \left( \frac{1}{1 + \frac{\partial \gamma_1}{\partial \bar{u}}(\bar{u})} \right). \tag{8}$$

Then, there exist  $G^* > 0$ ,  $t_0 > 0$ , and  $T > 0$  such that  $u(t) = \bar{u}(t) + O(1/G)$  for all  $t \in [t_0, T)$  and all  $G \geq G^*$ .

*Proof:* The proof proceeds similarly to the proof of Claim 1. Employ the change of variables  $\bar{u} := u + x_1$ ,  $\bar{x}_n = x_n + v_1$ , and set  $\epsilon := 1/G$ . The dynamics of system (4-5-6) in these new variables is the same as in equations (7). For  $\epsilon \ll 1$ , the above system is in standard singular perturbation form. Setting  $\epsilon = 0$ , one can compute the slow manifold in the  $(x, u)$  variables. This is given by  $\{(x, u) \mid x = \gamma(u), \text{ unique solution of } f(u, \gamma(u)) = 0\}$ . Denote the variables when  $\epsilon = 0$  with a bar. Then, we have that  $d\bar{u}/dt = f_0(t, \bar{u})$ . Since  $\bar{u} = \bar{u} + \bar{x}_1$ , by applying the chain rule we obtain

$$\frac{d\bar{u}}{dt} = f_0(t, \bar{u}) = \frac{d\bar{u}}{dt} + \frac{\partial \gamma_1}{\partial \bar{u}}(\bar{u}) \frac{d\bar{u}}{dt},$$

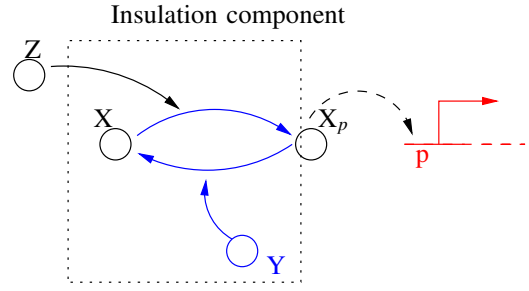


Fig. 4. The dashed box contains the insulation device.

which, rearranging the terms, leads to (8). Since all the eigenvalues of  $\frac{\partial F}{\partial x}(a, x)$  have negative real parts, we can apply the singular perturbation theorem on the finite time interval [14] to conclude that there are  $\epsilon^*, t_0, T > 0$  such that  $u(t) = \bar{u}(t) + O(\epsilon)$  for all  $\epsilon < \epsilon^*$  and  $t \in [t_0, T)$ . This leads us to the desired result with  $G^* = 1/\epsilon^*$ . ■

This result implies that if  $\frac{\partial \gamma_1}{\partial \bar{u}}(\bar{u}) \ll 1$  then the dynamics of  $u$  becomes, after a short transient and for  $G \geq G^*$ , approximately equal to  $\frac{d\bar{u}}{dt} = f_0(t, \bar{u})$ , which is the dynamics of  $u$  in the case in which  $r(x, u) = 0$ . Therefore, the quantity  $\frac{\partial \gamma_1}{\partial \bar{u}}(\bar{u})$  provides a measure of the retroactivity to the input  $r$  as a function of the input value and of the internal parameters of  $S$ . It can therefore be employed as a design parameter.

#### IV. AN INSULATION DEVICE REALIZATION BASED ON A PHOSPHORYLATION CYCLE

Consider a system  $S$  in which the input  $u$  is the concentration of a kinase  $Z$  that activates the phosphorylation of a protein  $X$  (Figure 4). Such a system can be designed to be an insulator by employing the method outlined in Section III.

##### A. Model and Design Criteria

Consider a two-step reaction model [11]:  $X + Z \xrightleftharpoons[\beta_2]{\beta_1} C_1 \xrightarrow{k_1} X_p + Z$  and  $Y + X_p \xrightleftharpoons[k_{off}]{\frac{k_{on}}{C_2}} C_2 \xrightarrow{k_2} X + Y$ , in which  $C_1$  is the [protein X/kinase Z] complex and  $C_2$  is the [phosphatase Y/protein  $X_p$ ] complex. Additionally, we have the conservation equations  $Y_{TOT} = Y + C_2$ ,  $X_{TOT} = X + X_p + C_1 + C_2 + C$ . Furthermore, we have  $X_p + p \xrightleftharpoons[k_{off}]{k_{on}} C$ , in which  $C$  is the complex protein-promoter and  $k_{on}$  and  $k_{off}$  are the binding and dissociation rates of  $X_p$  with  $p$ . Also, the total concentration  $p_{TOT}$  is conserved so that we can write  $p + C = p_{TOT}$ . The differential equations modeling the insulation system of Figure 4 become

$$\begin{aligned}
\frac{dZ}{dt} &= k(t) - \delta Z - \beta_1 Z X_{TOT} \left( 1 - \frac{X_p}{X_{TOT}} - \frac{C_1}{X_{TOT}} - \frac{C_2}{X_{TOT}} \right) \\
&\quad - \left( \frac{C}{X_{TOT}} \right) + (\beta_2 + k_1) C_1
\end{aligned} \tag{9}$$

$$\frac{dC_1}{dt} = -(\beta_2 + k_1)C_1 + \beta_1 ZX_{TOT} \left( 1 - \frac{X_p}{X_{TOT}} - \frac{C_1}{X_{TOT}} - \frac{C_2}{X_{TOT}} - \boxed{\frac{C}{X_{TOT}}} \right) \quad (10)$$

$$\frac{dC_2}{dt} = -(k_2 + \alpha_2)C_2 + \alpha_1 Y_{TOT} X_p \left( 1 - \frac{C_2}{Y_{TOT}} \right) \quad (11)$$

$$\frac{dX_p}{dt} = k_1 C_1 + \alpha_2 C_2 - \alpha_1 Y_{TOT} X_p \left( 1 - \frac{C_2}{Y_{TOT}} \right) + \boxed{k_{off}C - k_{on}X_p(p_{TOT} - C)} \quad (12)$$

$$\frac{dC}{dt} = -k_{off}C + k_{on}X_p(p_{TOT} - C), \quad (13)$$

in which the expression of gene  $z$  is controlled by a promoter with activity  $k(t)$ . The terms in the box in equation (9) represent the retroactivity  $r$  to the input, while the terms  $C/X_{TOT}$  in the small box in equation (9) and (10) and the box in equation (12) represent the retroactivity  $s$  to the output. We assume that  $X_{TOT} \gg p_{TOT}$  so that in equations (9) and (10) we can neglect the term  $C/X_{TOT}$  because  $C < p_{TOT}$  (note that this will in practice limit the load amount by the amount of  $X_{TOT}$ ). Phosphorylation, dephosphorylation, and binding dynamics can occur at a much faster rate [1], [13] than protein production and decay processes. That is,  $k_{off} \gg k(t)$ ,  $k_{off} \gg \delta$  [1], and  $k_{on} = k_{off}/k_d$  with  $k_d = \mathcal{O}(1)$ . Choosing  $X_{TOT}$  and  $Y_{TOT}$  sufficiently large, system (9–13) is in the form of system (4-6-5) in which  $x = (x_1, x_2, x_3) = (C_1, C_2, X_p)$ . This can be seen by letting  $G = k_{off}/\delta$ ,  $k_{on} = k_{off}/k_d$ , and by defining the new rate constants  $b_1 = (\beta_1 X_{TOT})/(\delta G)$ ,  $a_1 = (\alpha_1 Y_{TOT})/(\delta G)$ ,  $b_2 = \beta_2/(\delta G)$ ,  $a_2 = \alpha_2/(\delta G)$ ,  $c_i = k_i/(\delta G)$ , so to obtain the new system

$$\begin{aligned} \frac{dZ}{dt} &= k(t) - \delta Z \left( -\delta b_1 G Z \left( 1 - \frac{X_p}{X_{TOT}} - \frac{C_1}{X_{TOT}} - \frac{C_2}{X_{TOT}} \right) + G\delta(b_2 + c_1)C_1 \right) \\ \frac{dC_1}{dt} &= -G\delta(b_2 + c_1)C_1 + G\delta b_1 Z \left( 1 - \frac{X_p}{X_{TOT}} - \frac{C_1}{X_{TOT}} - \frac{C_2}{X_{TOT}} \right) \\ \frac{dC_2}{dt} &= -G\delta(c_2 + a_2)C_2 + G\delta a_1 X_p \left( 1 - \frac{C_2}{Y_{TOT}} \right) \\ \frac{dX_p}{dt} &= G\delta c_1 C_1 + G\delta a_2 C_2 - G\delta a_1 X_p \left( 1 - \frac{C_2}{Y_{TOT}} \right) + \boxed{G\delta C - G\delta/k_d(p_{TOT} - C)X_p} \\ \frac{dC}{dt} &= -G\delta C + G\delta/k_d(p_{TOT} - C)X_p, \end{aligned} \quad (14)$$

in which the boxed terms in the first equation are the retroactivity to the input  $r$ , while the boxed terms in the almost last equation are the retroactivity to the output  $s$ .

It can be shown that system (14) satisfies Assumption 1 provided  $X_{TOT}$  is large enough. Claim 1 can thus be applied: for  $G$  sufficiently large, we have that  $\|X_p(t) - X_p^r(t)\| = \mathcal{O}(1/G)$  after a short initial transient, in which  $X_p^{ref}(t)$  is the  $X_p(t)$  originating from (14) once we set  $s = 0$ . According to

this Claim 2, the function  $d\gamma_1(\bar{Z})/d\bar{Z}$  can be considered as a design parameter that should be made small in order to guarantee the retroactivity to the input  $r$  to be small after a short initial transient. To apply Claim 2, we next compute the expressions  $(C_1, C_2, X_p)$  as functions of  $Z$ . Letting  $\gamma = (\beta_2 + k_1)/\beta_1$  and  $\bar{\gamma} = (\alpha_2 + k_2)/\alpha_1$ , the following relationships can be obtained:

$$C_1 = F_1(X_p) = \frac{X_p Y_{TOT} k_2}{\bar{\gamma} k_1 (1 + X_p/\bar{\gamma})}, \quad C_2 = F_2(X_p) = \frac{X_p Y_{TOT}}{1 + X_p/\bar{\gamma}}, \quad (15)$$

$$F_1(X_p)(b_2 + c_1 + \frac{b_1 Z}{X_{TOT}}) = b_1 Z \left( 1 - \frac{X_p}{X_{TOT}} - \frac{F_2(X_p)}{X_{TOT}} \right). \quad (16)$$

Assuming for simplicity that  $X_p \ll \bar{\gamma}$ , we obtain that  $F_1(X_p) \approx (X_p Y_{TOT} k_2)/(\bar{\gamma} k_1)$  and that  $F_2(X_p) \approx (X_p Y_{TOT})/(\bar{\gamma})$ . As a consequence of these simplifications, equation (16) leads to

$$X_p = \frac{b_1 Z}{\frac{b_1 Z}{X_{TOT}} (1 + Y_{TOT}/\bar{\gamma} + (Y_{TOT} k_2)/(\bar{\gamma} k_1)) + \frac{Y_{TOT} k_2}{\bar{\gamma} k_1} (b_2 + c_1)}.$$

In order not to have distortion from  $Z$  to  $X_p$ , we require that

$$Z \ll \frac{Y_{TOT} \frac{k_2}{\bar{\gamma}}}{1 + \frac{Y_{TOT}}{\bar{\gamma}} + \frac{Y_{TOT} k_2}{\bar{\gamma} k_1}}, \quad (17)$$

so that  $X_p \approx Z \frac{X_{TOT} \bar{\gamma} k_1}{Y_{TOT} \bar{\gamma} k_2} := m(Z)$  and therefore we have a linear relationship between  $X_p$  and  $Z$  with gain from  $Z$  to  $X_p$  given by  $\frac{X_{TOT} \bar{\gamma} k_1}{Y_{TOT} \bar{\gamma} k_2}$ . In order not to have attenuation from  $Z$  to  $X_p$  we require that the gain is greater than or equal to one.

In order to guarantee that the retroactivity  $r$  to the input is sufficiently small, we require that the value of  $\partial F_1(m(Z))/\partial Z$  is small. Employing the chain rule, direct computation of  $\frac{dF_1}{dm}$  and of  $\frac{dm}{dZ}$  considering the expressions  $F_1(m) \approx \frac{m Y_{TOT} k_2}{\bar{\gamma} k_1}$  and  $m(Z) = Z \frac{X_{TOT} \bar{\gamma} k_1}{Y_{TOT} \bar{\gamma} k_2}$  leads to  $\partial F_1(m(Z))/\partial Z \approx X_{TOT}/\bar{\gamma}$ . Thus, in order to have small retroactivity to the input  $r$ , we require that  $\frac{X_{TOT}}{\bar{\gamma}} \ll 1$ .

## B. Simulation Results

A first validation of the proposed analysis is performed by using numerical integration of the differential equations (9–13) with and without the downstream binding sites  $p$ , that is, with and without, respectively, the terms in the small box of equation (9) and in the boxes in equations (12) and (10). This is performed to highlight the effect of the retroactivity to the output  $s$  on the dynamics of  $X_p$ . The simulations validate our theoretical study that indicates that when  $X_{TOT} \gg p_{TOT}$  and the time scales of phosphorylation/dephosphorylation are much faster than the time scale of decay and production of the protein  $Z$ , the retroactivity to the output  $s$  is very well attenuated (Figure 5, plot A). The accordance of the behaviors of  $Z(t)$  with and without its downstream binding sites on  $X$  (Figure 5, plot B), indicates that there is no substantial retroactivity to the input  $r$  generated by the insulation device. This is obtained because  $X_{TOT} \ll \bar{\gamma}$ , in which  $1/\bar{\gamma}$  can be interpreted as the affinity of the binding of  $X$  to  $Z$ . Our simulation study confirms that slowing down the time scale of phosphorylation and dephosphorylation, the system loses its insulation property (Figure 6).



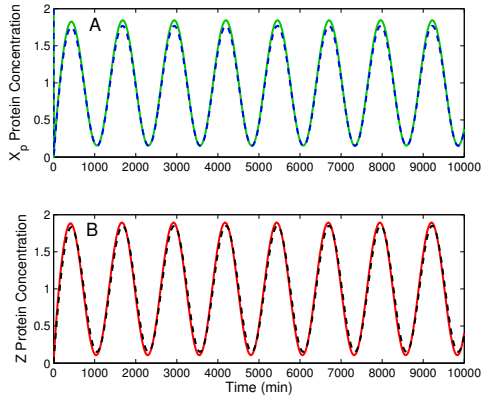


Fig. 5. Fast time scales of phosphorylation reactions. Simulation results for system in equations (9–13). In all plots,  $p_{TOT} = 100$ ,  $k_{off} = k_{on} = 10$ ,  $\delta = 0.01$ ,  $k(t) = 0.01(1 + \sin(\omega t))$ , and  $\omega = 0.005$ . In subplots A and B,  $k_1 = k_2 = 50$ ,  $\alpha_1 = \beta_1 = 0.01$ ,  $\beta_2 = \alpha_2 = 10$ , and  $Y_{TOT} = X_{TOT} = 1500$ . In subplot A, the signal  $X_p(t)$  without the downstream binding sites  $p$  is in green (solid line), while the same signal with the downstream binding sites  $p$  is in blue (dashed line). In subplot B, the signal  $Z(t)$  without  $X$  to which  $Z$  binds is in red (solid), while the same signal  $Z(t)$  with  $X$  present in the system ( $X_{TOT} = 1500$ ) is in black (dashed line).

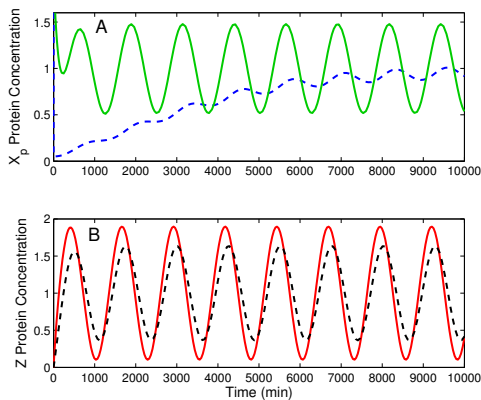


Fig. 6. Slower time scales of phosphorylation reactions. In all plots,  $p_{TOT} = 100$  and  $k_{off} = k_{on} = 10$ ,  $\delta = 0.01$ ,  $k(t) = 0.01(1 + \sin(\omega t))$ , and  $\omega = 0.005$ . Phosphorylation and dephosphorylation rates are slower than the ones in Figure 5, that is,  $k_1 = k_2 = 0.01$ , while the other parameters are left the same, that is,  $\alpha_2 = \beta_2 = 10$ ,  $\alpha_1 = \beta_1 = 0.01$ , and  $Y_{TOT} = X_{TOT} = 1500$ . In subplot A, the signal  $X_p(t)$  without the downstream binding sites  $p$  is in green (solid line), while the same signal with the downstream binding sites  $p$  is in blue (dashed line). In subplot B, the signal  $Z(t)$  without  $X$  in the system is in red (solid line), while the same signal  $Z(t)$  with  $X$  in the system is in black (dashed line).

## V. THE EFFECT OF BIOLOGICAL NOISE

### A. Simulation Model

For evaluating the noise properties of the phosphorylation system, we employed the Stochastic Simulation Algorithm (SSA) [7] using the Gillespie's direct method. SSA is appropriate in studies where the system satisfies properties of homogeneity of the solution, constant temperature and the

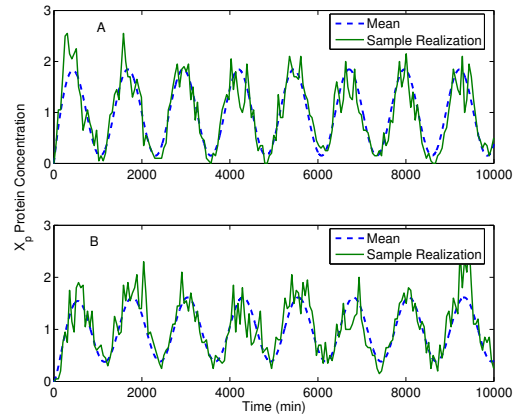


Fig. 7. Stochastic simulation realizations and sample mean for protein  $X_p$ . All results were obtained by using parameters  $k_{off} = k_{on} = 10$ ,  $\delta = 0.01$ ,  $k(t) = 0.01(1 + \sin \omega t)$ ,  $\omega = 0.005$ ,  $\alpha_1 = \beta_1 = 0.01$ ,  $\beta_2 = \alpha_2 = 10$ , and  $Y_{TOT} = X_{TOT} = 1500$ . The values of  $k_1$  and  $k_2$  are 0.05 in subplot A and 50 in subplot B. Both plots shown are for the system without load ( $p = 0$ ). When  $k_1$  and  $k_2$  are higher (subplot B),  $X_p$  comes close to zero, raising the maximum coefficient of variation.

proportion of non-reactive collisions is large. Under these assumptions, each realization of the method is equivalent to a sample of the random process described by the chemical master equation [8]. Our SSA implementation was modified to account for the time variant external input. This was accomplished by imposing a deterministic time-varying concentration for a  $Z$  protein messenger emulating the signal  $k(t) = 0.01(1 + \sin \omega t)$ . Here, we analyze the sensitivity of noise to changes in load and in a key parameter of this system. The measure used in this work to represent noise is the Coefficient of Variation (CV), obtained by taking the ratio between the standard deviation value of a species and its mean. This quantity, standard in biochemical assessment of noise [3], [10], is equal to the inverse square root of the signal-to-noise ratio. The importance of this measure comes from the fact that a high standard deviation value might have much higher impact on the overall dynamics when a species is scarce (present in low amounts) than when it is abundant in the system. The phosphorylation system shown in Figure 4 is, for the purpose of stochastic simulation, broken down into the set of corresponding chemical equations. The stochastic reaction rates used were chosen to be equivalent to those in the simulations from Section IV. The same initial conditions used in numerical integration were applied in the stochastic model, with concentrations converted into number of proteins by considering a system of volume  $\Omega = 20M^{-1}$ . Parameters  $K = k_1 = k_2$  and  $p$  were changed to assess noise sensitivity to gain and feedback, and to load. For each set of parameters, a total of  $N = 150$  realizations, denoted  $x_i(t)$  with length 10000s were generated. Sample realizations and means for the output  $X_p$  are shown in Figure 7.

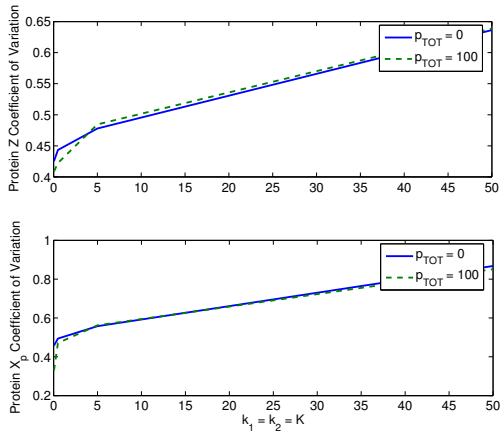


Fig. 8. Maximum coefficient of variation for input  $Z$  and output  $X_p$  in function of reaction rates  $k_1$  and  $k_2$ , for the system with and without load. This plot shows that increase in  $k_1$  and  $k_2$  lead to an increase in noise while load does not produce significant change.

### B. Stochastic Results and Analysis

Let the sample mean be  $\bar{x}(t) = \frac{1}{N} \sum_{i=0}^N x_i(t)$  and the biased variance estimator be  $\hat{\sigma}^2(t) = \frac{1}{N} \sum_{i=0}^N x_i^2(t)$ . Then the coefficient of variation is defined as  $CV(t) = \frac{\sqrt{\hat{\sigma}^2(t) - \bar{x}^2(t)}}{\bar{x}(t)}$ . In this work, we are interested in the maximum coefficient of variation for the proteins  $Z$  and  $X_p$  over time. These were obtained by using the expression  $\overline{CV} = \max_{t > \bar{t}} CV(t)$ , in which  $\bar{t} > 0$  is chosen as  $\bar{t} = 2000$  in order to exclude the transient from the computation of  $\overline{CV}$ . Figure 8 shows the maximum coefficient of variation on input ( $Z$ ) and output ( $X_p$ ) for  $K = 0.05, 0.5, 5, 50$  and  $p_{TOT} = 0, 100$ . The maximum coefficient of variation on both input and output states was not significantly affected when downstream load is connected. When  $K$  is increased, the noise on both states increases dramatically, the output state suffering the most. This fact along with the results from Section IV points at a trade-off between the performance of the insulator and the noise produced by it. The value of  $K$  should not be too low so that the system can efficiently reduce the retroactivity to the output, nor too high to avoid a large coefficient of variation. It has been shown that the increase of feedback leads to increase in high frequency noise sensitivity and might lead to instability of systems with additive noise [5]. This fundamental principle is not directly applicable to our system because the perturbations are not additive and are correlated to the states. The effects of feedback increase on noise have been investigated by some authors for systems at the equilibrium [3], [10]. While the first of these works shows how negative feedback may decrease the CV in a simple autoregulated gene, the second one shows that the addition of negative feedback not necessarily decreases the CV. Our findings are more in line with the results of [10] even if not directly comparable as our system is not at the equilibrium due to a time varying input. A study of the effect of feedback on noise has been investigated for systems out

of equilibrium in [19], supporting the possibility that noise may not be decreased by feedback when the state is far from equilibrium. This result is closer to our finding, even if our system operates in the permanent (non-steady) behavior as opposed to operate in the transient behavior.

## VI. CONCLUSIONS AND FUTURE WORK

We described a methodology based on singular perturbation analysis for the design of insulation devices in transcriptional networks. We then proposed a specific design of an insulation device based on a phosphorylation cycle. On the one side, as the gain  $G$  increase the insulation property improves. On the other side an increase in this gain causes an increase in biological noise. This result points at a design tradeoff. We are investigating analytically the reasons for an increase in noise due to an increase in gain. The proposed insulation device will be fabricated in *E. coli* to experimentally validate our theoretical analysis.

## REFERENCES

- [1] U. Alon. *An introduction to systems biology. Design principles of biological circuits*. Chapman-Hall, 2007.
- [2] M. R. Atkinson, M. A. Savageau, J. T. Meyers, and A. J. Ninfa. Development of genetic circuitry exhibiting toggle switch or oscillatory behavior in *Escherichia coli*. *Cell*, pages 597–607, 2003.
- [3] A. Becskei and L. Serrano. Engineering stability in gene networks by autoregulation. *Nature*, 405:590–593, 2000.
- [4] H. C. Berg. The rotary motor of bacterial flagella. *Annual Review of Biochemistry*, 72:19–54, 2003.
- [5] H. W. Bode. *Network Analysis and Feedback Amplifier Design*. Van Nostrand, 1945.
- [6] D. Del Vecchio, A. J. Ninfa, and E. D. Sontag. Modular cell biology: Retroactivity and insulation. *Nature/EMBO Molecular Systems Biology*, 4(161), 2008.
- [7] D. T. Gillespie. Exact stochastic simulation of coupled chemical reactions. *The Journal of Physical Chemistry*, 81:2340–2361, 1977.
- [8] D. T. Gillespie. A rigorous derivation of the chemical master equation. *Physica A*, 188:404–425, 1992.
- [9] L.H. Hartwell, J.J. Hopfield, S. Leibler, and A.W. Murray. From molecular to modular cell biology. *Nature*, 402:47–52, 1999.
- [10] S. Hooshangi and R. Weiss. The effect of negative feedback on noise propagation. *Chaos*, 16, 2006.
- [11] C. F. Huang and J. E. Ferrell. Ultrasensitivity in the mitogen-activated protein kinase cascade. *Proc. Natl. Acad. Sci.*, 93(19):10078–10083, 1996.
- [12] T. Hunter. Protein kinases and phosphatases: The yin and yang of protein phosphorylation and signaling. *Cell*, 80:225–236, 1995.
- [13] B. N. Kholodenko, G. C. Brown, and J. B. Hoek. Diffusion control of protein phosphorylation in signal transduction pathways. *Biochem. J.*, 350:901–907, 2000.
- [14] P. Kokotovic, H. K. Khalil, and J. O’Reilly. *Singular Perturbation Methods in Control*. SIAM, 1999.
- [15] J. W. Polderman and J. C. Willems. *Introduction to Mathematical Systems Theory. A Behavioral Approach. 2nd ed.* Springer-Verlag, New York, 2007.
- [16] J. Saez-Rodriguez, A. Kremling, H. Conzelmann, K. Bettenbrock, and E. D. Gilles. Modular analysis of signal transduction networks. *IEEE Control Systems Magazine*, pages 35–52, 2004.
- [17] H. M. Sauro and B. Ingalls. MAPK cascades as feedback amplifiers. Technical report, <http://arxiv.org/abs/0710.5195>, Oct 2007.
- [18] L. Stryer. Cyclic gmp cascade of vision. *Annual Review of Neuroscience*, 9:87–119, 1987.
- [19] Y. Tao, Y. Jia, and G. Dewey. Stochastic fluctuations in gene expression far from equilibrium:  $\Omega$  expansion and linear noise approximation. *Journal of Chemical Physics*, 122:124108, 2005.